

Consideration about the Energy Distribution of Fast Deuterons in the Plasma Focus Device

P. Kubes, J. Kravarik, D. Klir, K. Rezac, E. Litseva, M. Scholz, M. Paduch,
K. Tomaszewski, I. Ivanova-Stanik, B. Bienkowska, L. Karpinski,
M.J. Sadowski, H. Schmidt

CTU Prague, Technicka 2, 166 27 Prague, Czech Republic

*Institute of Plasma Physics and Laser Microfusion, 23 Hery, 00-908
Warsaw, Poland*

⁴ACS Warsaw Hery 23, 01-497 Warsaw Poland

Motivation

Formulation of the model
for generation of neutrons in Z-pinch discharges, of both
the dominant part of beam target,
and possible thermonuclear origin

Outline

Experimental and diagnostic set-up

Energy distribution of neutrons

Energy distribution of deuterons producing neutrons
in axial and side-on direction

Dimensions and densities of neutron sources

Energy distribution of all fast deuterons

Confinement of fast deuterons in magnetic field

Heating and cooling of the neutron source by i-i and e-i Coulomb collisions

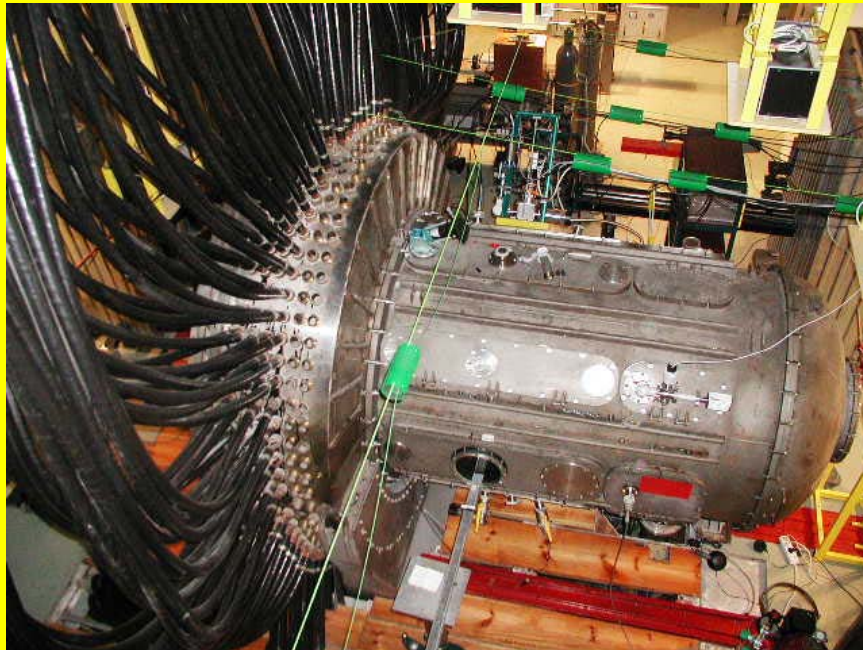
Conclusions

PF-1000 IPPLM Warsaw, Poland

2 MA, 400 kJ, D-D reaction, D₂ gas

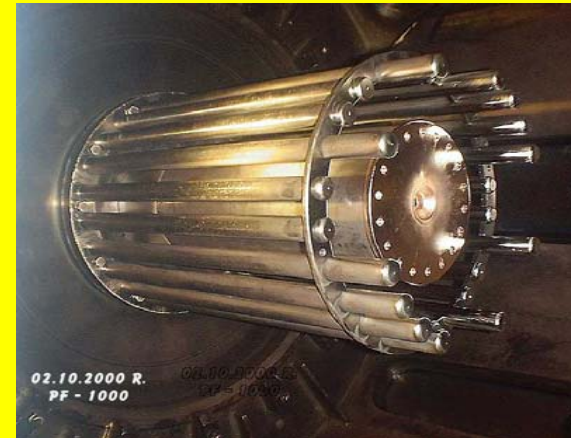
neutron yield 10¹⁰-10¹¹ , horizontal position of discharge axis

facility



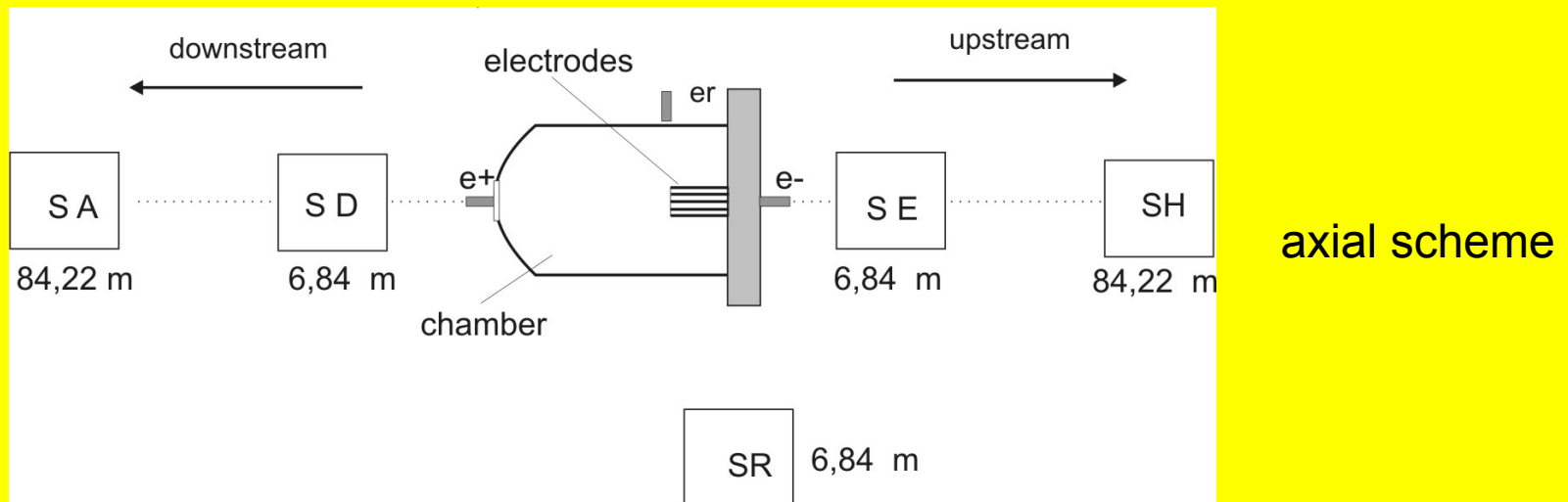
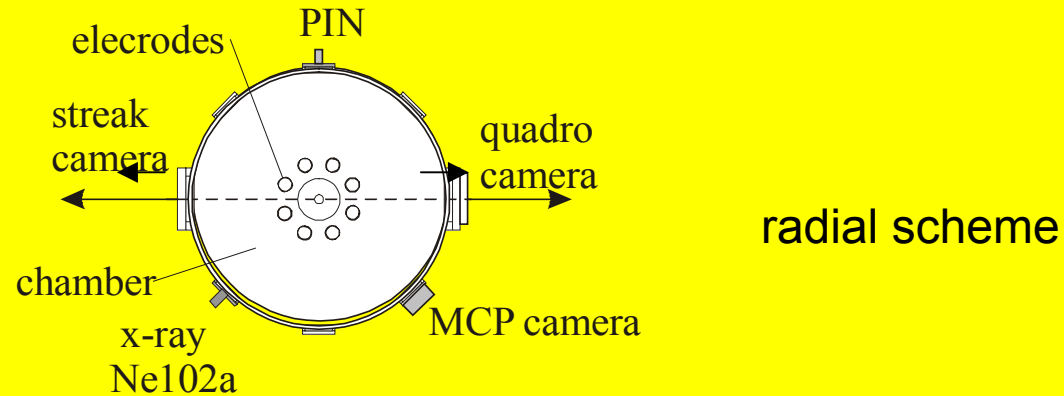
- volume ~ 3.8 m³
- Ø = 1.4 m
- L = 2.5 m

electrode system



- 8 rods
- Ø a = 230 mm
- Ø c = 400 mm
- L = 600 mm

Scheme of neutron diagnostics with temporal distribution

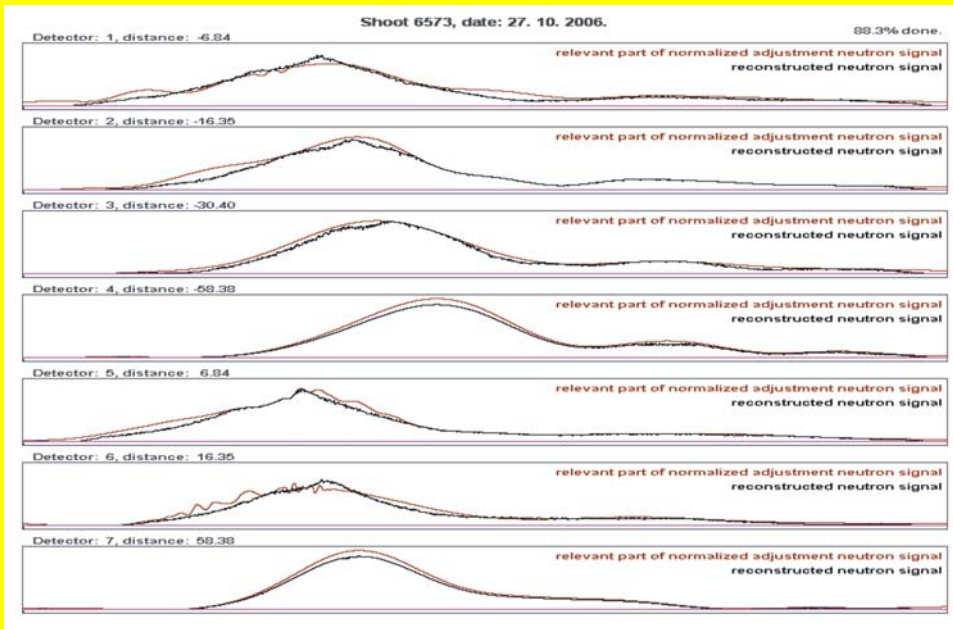


10 HXR and neutron scintillation detectors

Temporal evolution of neutron energies downstream

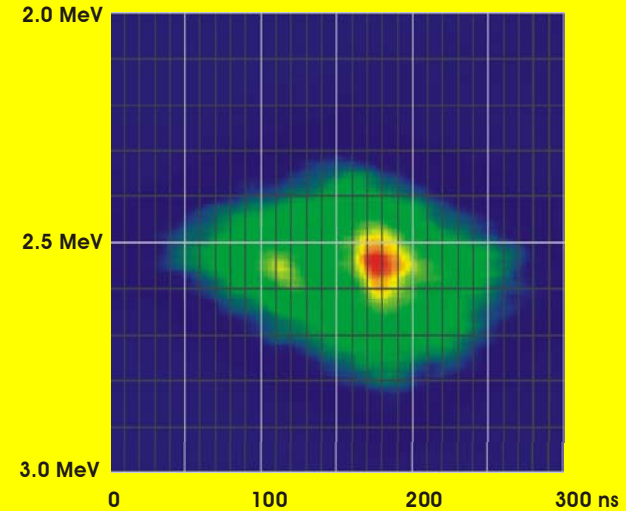
shot No. 6573 with total neutron yield 4×10^{10}

adapted time-of-flight and MC simulations $I_{\text{TOF}}(t_0, E)$

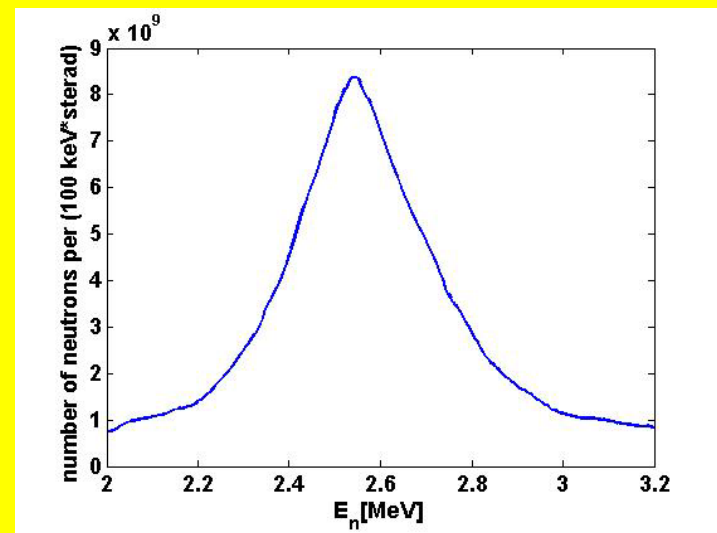


adaptation:

- transformation of neutron energy down/up
- corrections for anisotropy down/up
- dependance of the E_n on the E_d and angle



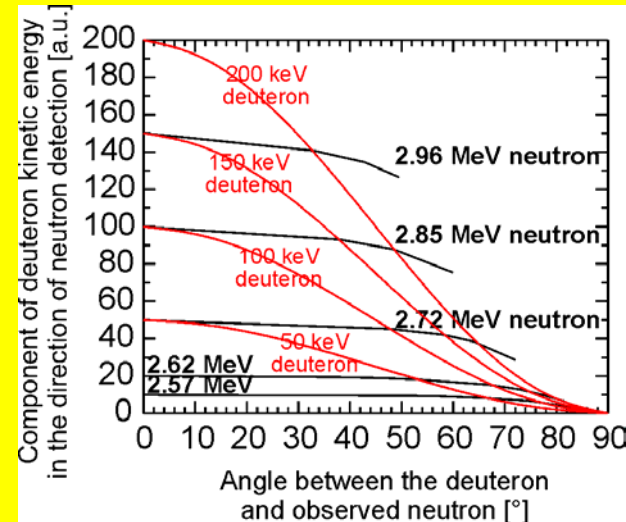
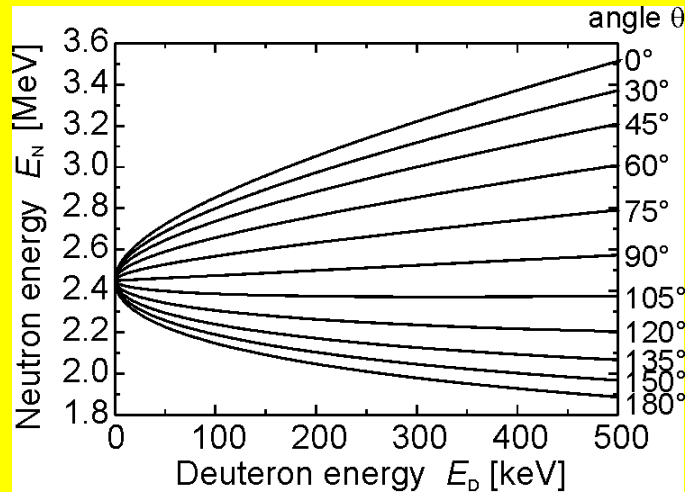
temporal evolution of neutron energies



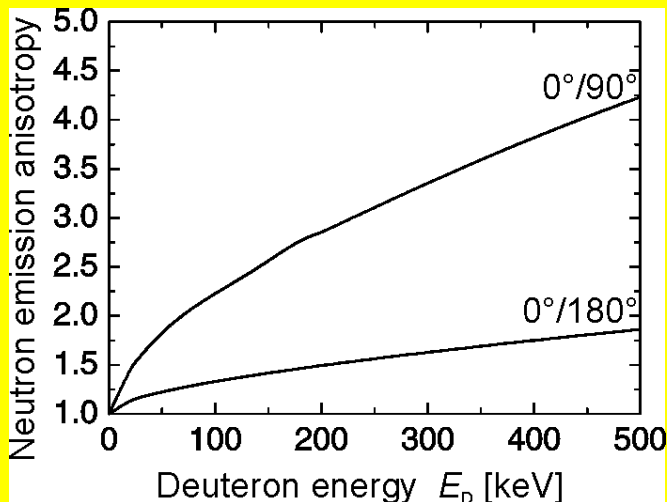
downstream distribution of
neutron energy per (100 keV)

Determination of the axial component of deuteron energy producing observed neutrons

a) transformation of neutron energy down/up

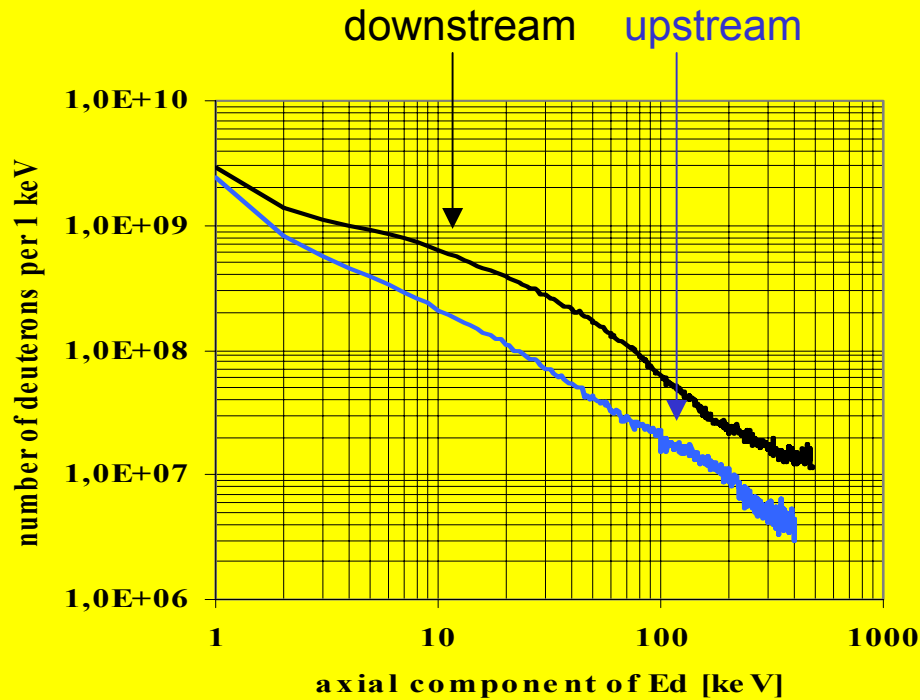


b) corrections for anisotropy down/up



c) dependance of the E_n on the E_D and angle between the deuteron and observed neutron

Determination of the axial component of deuteron energy producing observed neutrons



Shot 6573:

axial component of E_D producing neutrons

total No 4×10^{10}

$$N_D \sim E_D^{-1}$$

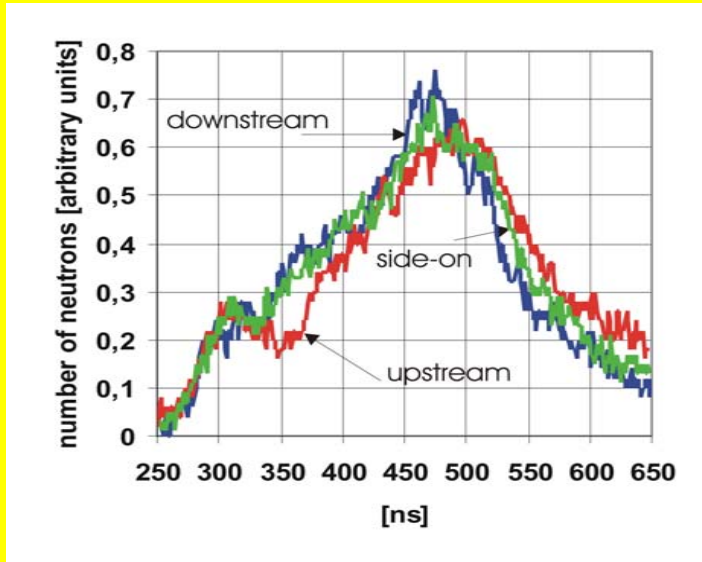
$$N_d/N_u \approx 2-3$$

Determination of the radial component of deuteron energy producing observed neutrons

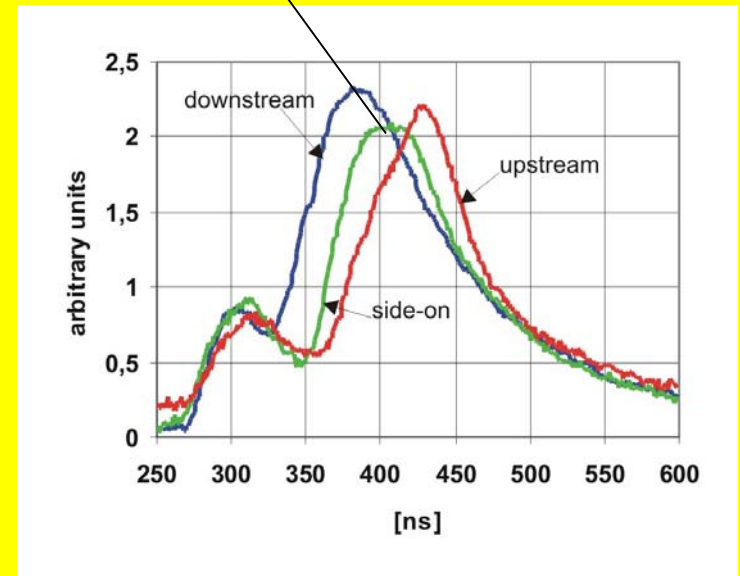
? radial distribution of neutron energies ?

We registered only in 7 m downstream, upstream and side-on; only partial energy distribution

high anisotropy for the shots with high neutron yield



Shot 6573; NY 4×10^{10} : axial and side-on neutron signals in 7 m

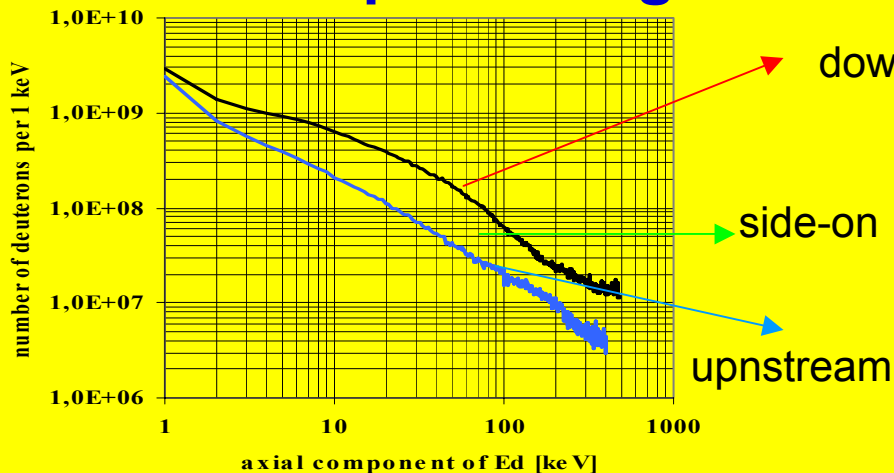


Shot 6552; NY 2×10^{11} : axial and side-on neutron signals in 7 m

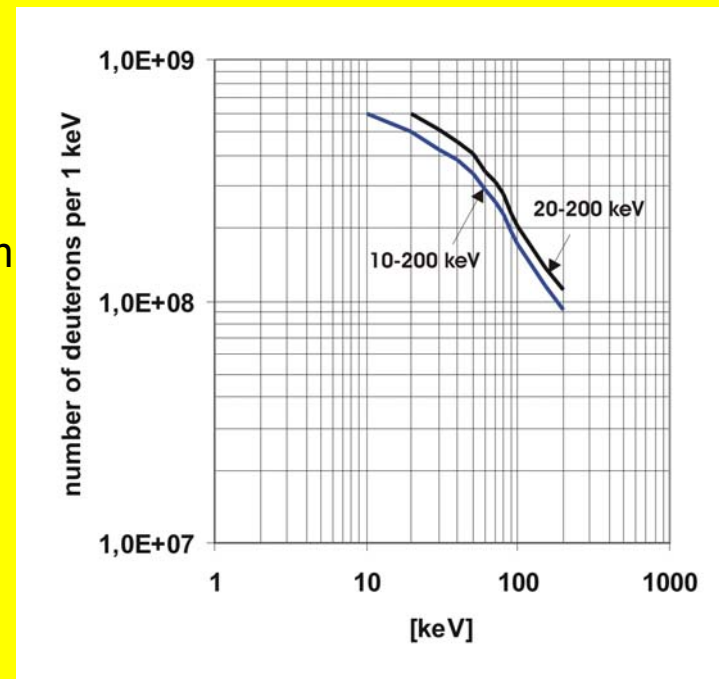
Supposition:

- isotropy distribution of deuteron velocities in the range below 100 keV in the shots with the lower neutron yield
- test of the lower limit of D producing neutrons 10, 20 keV

Determination of the deuteron energy producing observed neutrons

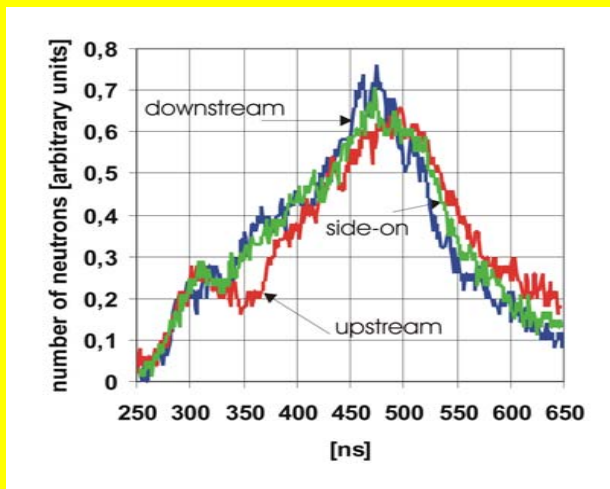


Shot 6573: axial component of deuteron energy producing neutrons



total energy distribution of deuterons producing neutrons; 4×10^{10}

variants 10; 20; keV



Shot 6573; NY 5×10^{10} : axial and side-on neutron signals in 7 m

Probability of the D-D fusion reaction

probability of D – D fusion collisions:

$$p_{DD} = l \lambda_{DD} = l n_i \sigma(E_d)$$

$\sigma(E_d)$... cross-section of D-D reaction ...

n_i ... deuteron density of the neutron source ...

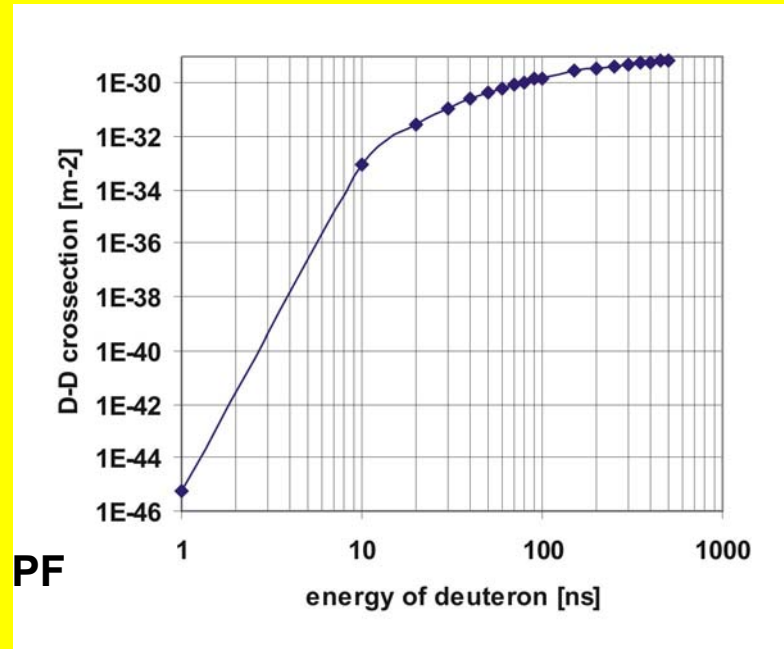
l ... length of the neutron source

dimensions of the source ... experimental data
Schmidt (2006), Sadowski (2006) ... < 10 cm

⇒ density of the source .. > 10^{25} m^{-3} .

source of neutrons - dense structures in the PF

⇒ surface density of the target $nl.. > 10^{24} \text{ m}^{-2}$.



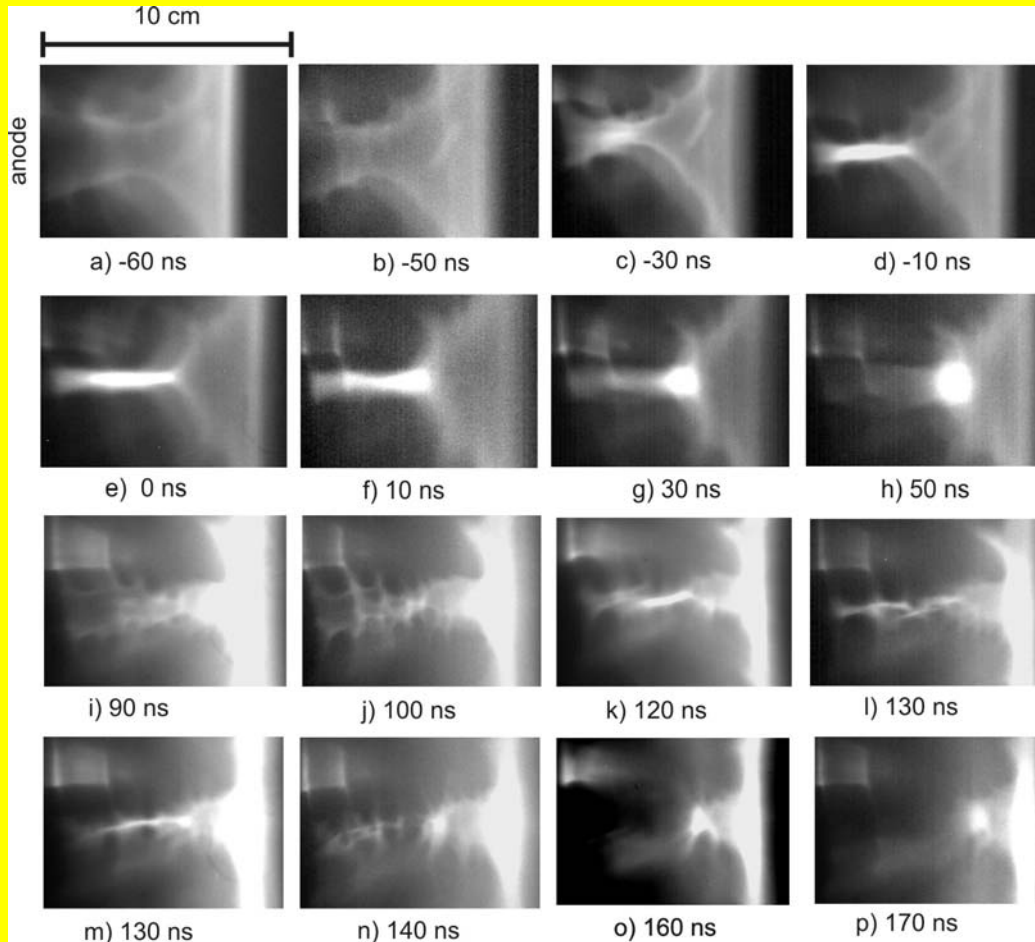
$\sigma(E_D)$ cross-section of D-D reaction

Dependence of the length on the density of the target for neutron yield of 10^{10} - 10^{11}

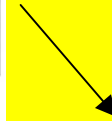
length	50 cm	5 cm	5 mm	0,5 mm
density	10^{24} m^{-3}	10^{25} m^{-3}	10^{26} m^{-3}	10^{27} m^{-3}

visual frames

Dense structures in the PF



→ first neutron peak (-10 – 50 ns)



→ second neutron peak 100-200 ns

supposition of the neutron source ... **length 2 cm, density $2 \times 10^{25} \text{ m}^{-3}$.**

Kubes P. et al: Correlation of Radiation with Electron and Neutron Signals Taken in a Plasma-Focus Device, IEEE TPS Vol. 34, Issue 5, Part 3, Oct. 2006, pp. 2349-2355.

Mean path of DD reaction; $\lambda_{DD} = 1/n \cdot \sigma(E)$, [m]

ni m ⁻³	10 keV	20 keV	50 keV	100 keV	150 keV	200 keV
10 ²⁷	1x10 ⁵	3.6x10 ⁴	2.2x10 ³	6.2x10 ²	3.7x10 ²	2.8x10 ²
10 ²⁶	1x10 ⁶	3,6x10 ⁵	2.2x10 ⁴	6.2x10 ³	3.7x10 ³	2.8x10 ³
10 ²⁵	1x10 ⁷	3.6x10 ⁶	2.2x10 ⁵	6.2x10 ⁴	3.7x10 ⁴	2.8x10 ⁴
10 ²⁴	1x10 ⁸	3.6x10 ⁷	2.2x10 ⁶	6.2x10 ⁵	3.7x10 ⁵	2.8x10 ⁵
10 ²³	1x10 ⁹	3.6x10 ⁸	2.2x10 ⁷	6.2x10 ⁶	3.7x10 ⁶	2.8x10 ⁶

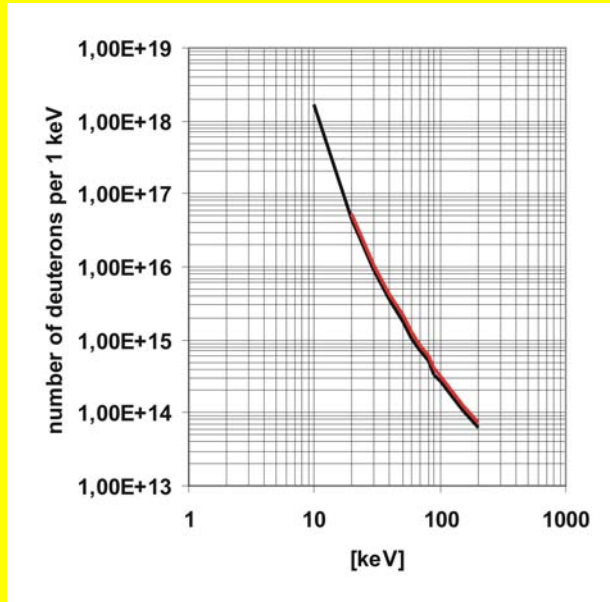
Evaluation of the deuteron energy distribution

Supposition:

isotropy distribution of d velocities

target - l = 2 cm, density = $2 \times 10^{25} \text{ m}^{-3}$

TABLE I: TOTAL VALUES OF FAST DEUTERONS



Ed [keV]	Number of deuterons	E _{total} [kJ]	I _{total} [kA]
10 - 200	9×10^{18}	17	300
20 - 200	10^{18}	10	140
30 - 200	2.5×10^{17}	1.7	70
1 - (10-20)	10^{19}	20	350

Shot 6573: distribution of energy of deuterons producing neutrons

	100 keV ...	10^{16}
	50 keV ...	10^{17}
Total number of deuterons with energy above	20 keV ...	10^{18}
	10 keV ...	10^{19}

Confinement of the deuterons in magnetic field

distribution of deuteron velocities: downstream 50 %, side-on 30-40%, upstream 10-20%
is it possible change the direction of the fast deuterons by internal magnetic field?

$$B = \mu I / 2\pi r_p = mv / er_L \Rightarrow I = 2\pi mv / e\mu \Rightarrow v = I e\mu / 2\pi m;$$

E_d	10 keV	30 keV	100 keV	300 keV
v	10^6 m/s	1.7×10^6 m/s	3×10^6 m/s	5×10^6 m/s
path 100ns	10 cm	15 cm	30 cm	100 cm
I	4×10^5 A	7×10^5 A	1.2×10^6 A	4×10^6 A

The path of the fast deuterons can increase and their velocities can be changed by internal magnetic field;

Cooling of the deuterons and heating of electrons by Coulomb interaction with fast deuterons

Relaxation time of Coulomb i-i collisions

$$\tau_{ii} = \frac{\lambda_{ii}}{\nu_i} = \frac{4.5 \times 10^{17} T^{3/2}}{5.9 \times 10^5 n \ln \Lambda} \left(\frac{M}{m} \right)^{1/2}$$

τ_{ii} [ns]	0.5 keV	1 keV	2 keV	5 keV	10 keV	20 keV
1E27 m ⁻³	0.05	0.14	0.39	1.6	4.4	13
1E26 m ⁻³	0.5	1.4	3.9	15.6	44	130
1E25 m ⁻³	5	14	39	156	440	1300
1E24 m ⁻³	50	140	390	1560	4400	13000

Relaxation time of Coulomb e-i collisions

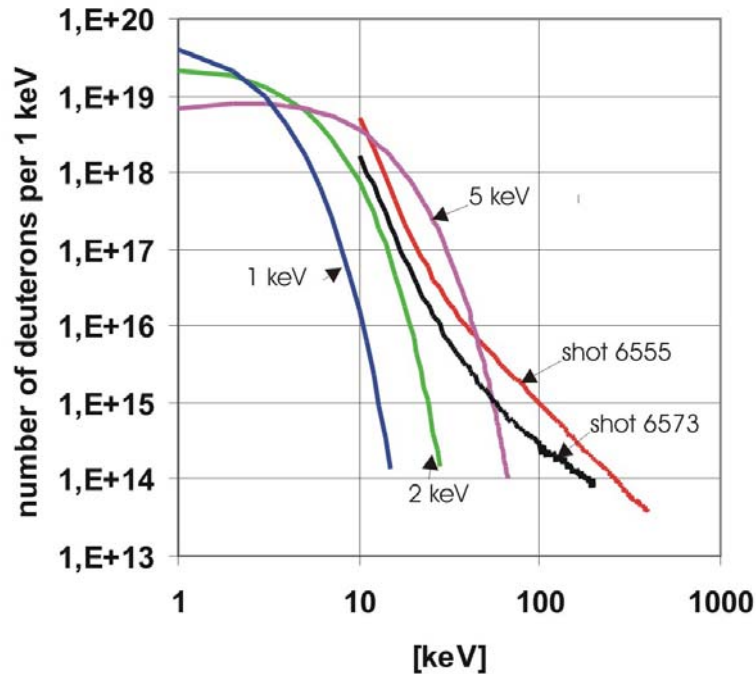
$$\tau_{ie} = \tau_{ii} \sqrt{\frac{M}{m}} \left(\frac{T_E}{E_i} \right)^{3/2} = 7.6 \times 10^{12} \sqrt{\frac{M}{m}} \frac{T_i^{3/2}}{n \ln \Lambda} \cdot \sqrt{\frac{M}{m}} \left(\frac{T_E}{E_i} \right)^{3/2} = 7.6 \times 10^{12} \frac{M}{m} \frac{T_e^{3/2}}{n \ln \Lambda}$$

Te [ns]	0.1 keV	0.3 keV	1 keV	3 keV		
1E27 m ⁻³	0.27	1.5	8.5	44		
1E26 m ⁻³	2.7	15	85	440		
1E25 m ⁻³	27	150	850	4400		
1E24 m ⁻³	270	1500	8500	44000		

independently
on the Ed

In the localities with the density 10²⁵ m⁻³ an effective heating of deuterons with i-i collisions up to 1-2 keV and effective cooling with e-i collisions to the temperature 0.1 keV.

Maxwellian and experimental deuteron energy distribution



Possibility of heating of the
dense structures to the
temperatures:

Ti ... 2 keV

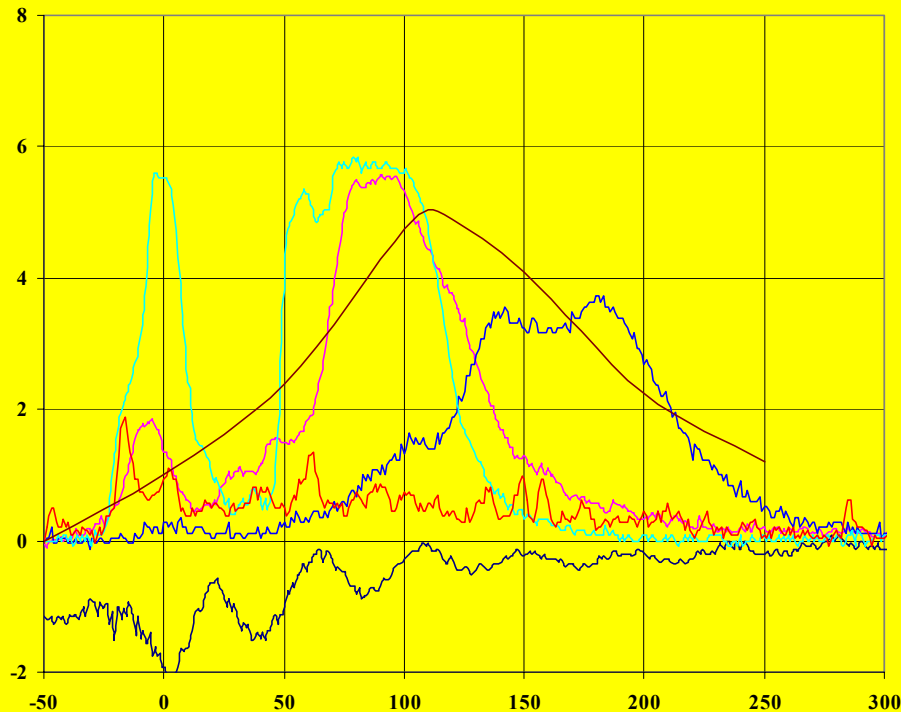
Te ... 100-200 eV

with i-i collisions of deuterons
with energies in the range of
1-20 keV

Comparisson of experimental and
Maxwellian E_D

Spherical structure can be heated to the T_i 1-2 keV and T_e 100 eV

Experimental support



fast electrons

HXR above 100 keV

neutrons

XR above 10 keV

current derivative

shot 6555

The plasma can be heated by fast deuterons to the high electron temperature

Conclusions

The dense spherical structure with the n_i above 10^{25} m^{-3} can be the neutron source.

This structure can be heated with Coulomb collisions to the T_i of 1-2 keV and T_e 100-200 eV.

Energy distribution of fast deuterons has non-Maxwell high-energy tail.

The magnetic field in the structure can confine the deuterons with energies up to 10-20 keV and change the path of the part of deuterons with energy above 20 keV.

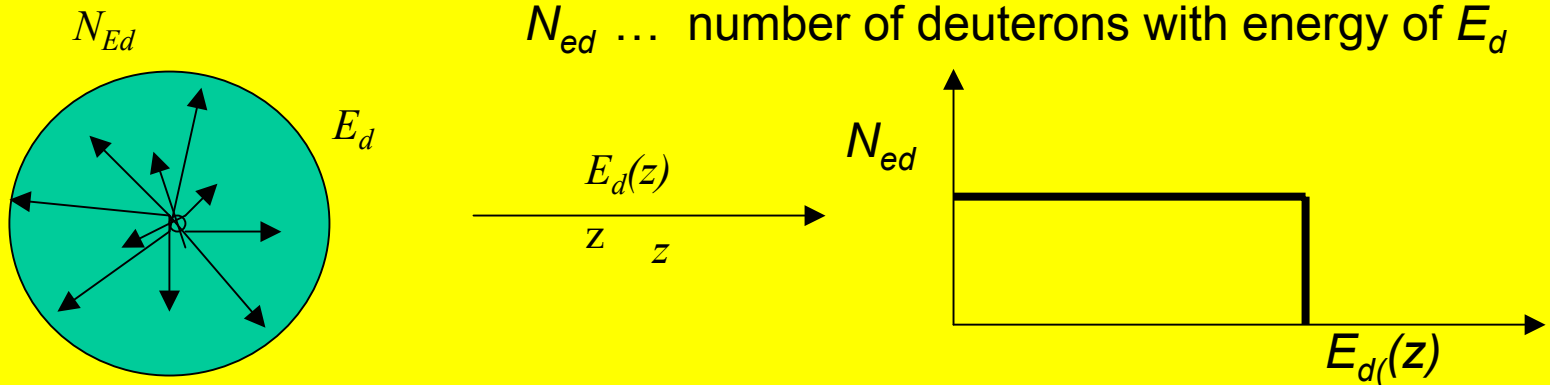
The number of thermonuclear neutrons can be 10^7 - 10^9 .

For more detail analysis we plan in this year installation of: neutron scintillation detectors side-on in distances 2 and 50 m, laser interferometry with 4-8 frames per shot and later measurements of magnetic field.

We will continue the study of the TOF analysis of neutrons (K. Řezac), of energy transformation in the pinch (D. Klir) and of the influence of the magnetic field on the dynamics of the pinch (M. Bohata).

Determination of energy distribution of deuterons from the known component in one direction (z)

1. for monoenergy deuterons with isotropy distribution of velocities



$$\Delta N_{Ed} [1 keV] = \frac{N_{Ed}}{4\pi} \Delta S = \frac{N_{Ed}}{4\pi} \frac{N_{Ed}}{4\pi} \int_0^{2\pi} \int_0^{2\pi} E_d^2 \sin \theta d\phi \Delta\theta = \frac{N_{Ed}}{4\pi} \int_0^{2\pi} E_d^2 \sin \theta d\phi \frac{d\theta}{dz} \Delta z = \left(\frac{d\theta}{dz} = \frac{1}{E_d \sin \theta} \right) = \frac{N_{Ed}}{E_d} \Delta z [1 keV]$$

This dependence is constant along the range of 0- E_d

2. Transformation of the axial energy component to the total energy – factor $(E_d)^{1/2}$

$$f(E) = f(v) \cdot \frac{dv}{dE} = f(v_s) \cdot 4\pi v^2 \cdot (2mE)^{-1/2} = f(v_z) \cdot 8\pi (2/m)^{-1/2} \cdot E^{1/2} \sim f(E_z) \cdot E^{1/2}$$